

Molecular dynamics analysis of transitions between rotational isomers in polymethylene

Ignacio Zúñiga

Departamento de Física Fundamental, UNED, Apartado 60141, 28080 Madrid, Spain

Ivet Bahar

Department of Chemical Engineering and Polymer Research Center, Boğaziçi University, Bebek 80815, Istanbul, Turkey

Robert Dodge and Wayne L. Mattice

Institute of Polymer Science, The University of Akron, Akron, Ohio 44325-3909

(Received 27 September 1990; accepted 28 June 1991)

Molecular dynamics trajectories have been computed and analyzed for linear chains, with sizes ranging from $C_{10}H_{22}$ to $C_{100}H_{202}$, and for cyclic $C_{100}H_{200}$. All hydrogen atoms are included discretely. All bond lengths, bond angles, and torsion angles are variable. Hazard plots show a tendency, at very short times, for correlations between rotational isomeric transitions at bond i and $i \pm 2$, in much the same manner as in the Brownian dynamics simulations reported by Helfand and co-workers. This correlation of next nearest neighbor bonds in isolated polyethylene chains is much weaker than the correlation found for next nearest neighbor CH-CH₂ bonds in poly(1,4-*trans*-butadiene) confined to the channel formed by crystalline perhydrotriphenylene [Dodge and Mattice, *Macromolecules* **24**, 2709 (1991)]. Less than half of the rotational isomeric transitions observed in the entire trajectory for $C_{50}H_{102}$ can be described as strongly coupled next nearest neighbor transitions. If correlated motions are identified with successive transitions, which occur within a time interval of $\Delta t \leq 1$ ps, only 18% of the transitions occur through cooperative motion of bonds i and $i \pm 2$. An analysis of the entire data set of 2482 rotational isomeric state transitions, observed in a 3.7 ns trajectory for $C_{50}H_{102}$ at 400 K, was performed using a formalism that treats the transitions at different bonds as being independent. On time scales of 0.1 ns or longer, the analysis based on independent bonds accounts reasonably well for the results from the molecular dynamics simulations. At shorter times the molecular dynamics simulation reveals a higher mobility than implied by the analysis assuming independent bonds, presumably due to the influence of correlations that are important at shorter times.

I. INTRODUCTION

Transitions between rotational isomeric states play the dominant role in local relaxational phenomena in macromolecules. For common flexible polymers in solutions of low viscosity, the time scale of the motions is on the order of nanoseconds or less. This time scale is well suited for investigation by simulations of the molecular dynamics. The molecular dynamics technique has proven to be of great value in providing insights into both the equilibrium and dynamic behavior of biological molecules, in particular.¹ The purpose of the present work is to use the molecular dynamics technique to extract information on the kinetics of two fundamental processes, the rotational isomerization and equilibration, for an atom-based model of a common flexible polymer.

Polyethylene chains of n backbone bonds will be the system whose dynamics will be monitored in the present study. As far as the isomerization kinetics of real linear alkane chains is concerned, several important contributions²⁻¹⁷ employing Brownian/stochastic dynamics or equivalent approaches furnish reasonable quantitative information. In this respect, the type of conformational potential adopted is of major importance in prescribing the dynamic behavior. Various approaches have been adopted in previous work, including Fixman-Kovac² and Ryckaert-Bellemans³

models with holonomic constraints fixing all degrees of freedom other than torsional angles mobility, or Weber's method^{5,6} in which bond angles, as well, are subject to harmonic potentials, etc. Here we use a version of the CHARMM algorithm developed by Karplus¹³ and supplied by Polygen.¹⁸ The model considers all hydrogen atoms explicitly. All bond lengths, bond angles, and dihedral angles are variable. The probability distribution for ϕ_i, ϕ_{i+1} , evaluated over a trajectory sufficiently long for a thorough sampling of the ϕ_i, ϕ_{i+1} surface, is consistent with the familiar features found in the conformational energy surfaces of small linear alkanes.¹⁹

The results from simulations will be analyzed in relation to a simple model of rotameric transitions of backbone bonds, which is the basic mechanism of relaxation adopted in the dynamic rotational isomeric state approach.^{20,21} We will also look for sequential rotameric transitions at bonds i and $i \pm j$, where j is a small integer.

II. METHODOLOGY OF THE MOLECULAR DYNAMICS SIMULATIONS

The molecular dynamics simulations were performed with the CHARMM algorithm¹ using the CHARMM force field version 2.1A without electrostatics. Initial velocities for all of the hydrogen and carbon atoms were chosen according to

the Boltzmann distribution. The system was allowed to equilibrate for 100 ps before starting the analysis. Trajectories with time steps of 0.1, 0.5, and 1 fs were computed and compared. The results reported here are those obtained with a time step of 0.5 fs. This choice of time step gave the fastest convergence to equilibrium values. Structural variables were recorded at intervals of 100 fs. Every 500 fs the temperature was checked, and if it was more than ± 10 K from the desired temperature (300 or 400 K), the velocities were scaled by a single factor to bring the temperature into the desired range. Most of the simulations were performed with linear $C_{50}H_{102}$ at a temperature of 400 K. A few results were also obtained at 300 K in order to facilitate comparison with previous work. We also studied several other linear chains ranging in size from $C_{10}H_{22}$ to $C_{100}H_{202}$, and one cyclic chain, $C_{100}H_{200}$.

A small portion of a typical trajectory for an internal C–C bond at 400 K is depicted in Fig. 1. This trajectory shows very rapid oscillations of magnitude several tens of degrees, and less frequent jumps of magnitude near 120° . The range of the very rapid oscillations is better seen in Fig. 2, where we plot the probability distribution of dihedral angles for all internal C–C bonds. This distribution shows three peaks at the expected isomeric states, *trans* (*t*), *gauche*⁺ (*g*⁺), and *gauche*[−] (*g*[−]).

An analysis as probability vs ϕ_i and ϕ_{i+1} (not shown here, but presented as Fig. 5 of Bahar *et al.*²²) shows all of the features expected, based on the conformational energy surfaces computed for small linear alkanes.¹⁹ The molecular dynamics trajectory even reveals the splitting of the strongly suppressed *g*[±]*g*[∓] regions into two peaks of probability (derived from two closely spaced minima of conformational energy, as shown by Abe *et al.*¹⁹) separated by about 20° in ϕ_i and ϕ_{i+1} . Hence the force field in CHARMM produces a distribution of dihedral angles that is in excellent agreement with that expected on the basis of the rotational isomeric state analysis of polyethylene by Abe *et al.*¹⁹

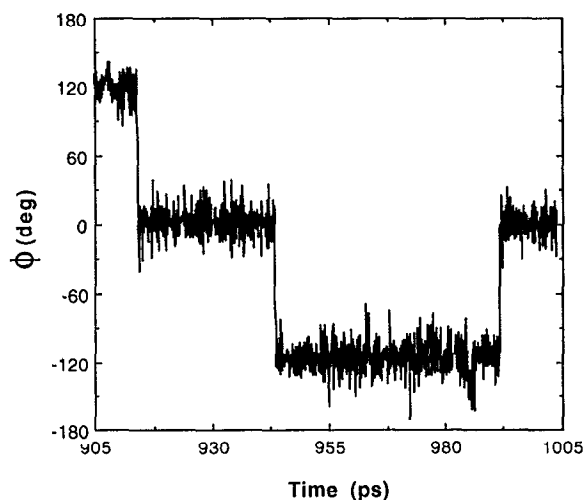


FIG. 1. Illustrative behavior of the dihedral angle, measured relative to $\phi = 0^\circ$ for a *t* state, at a typical internal C–C bond in a 100 ps section of a trajectory at 400 K.

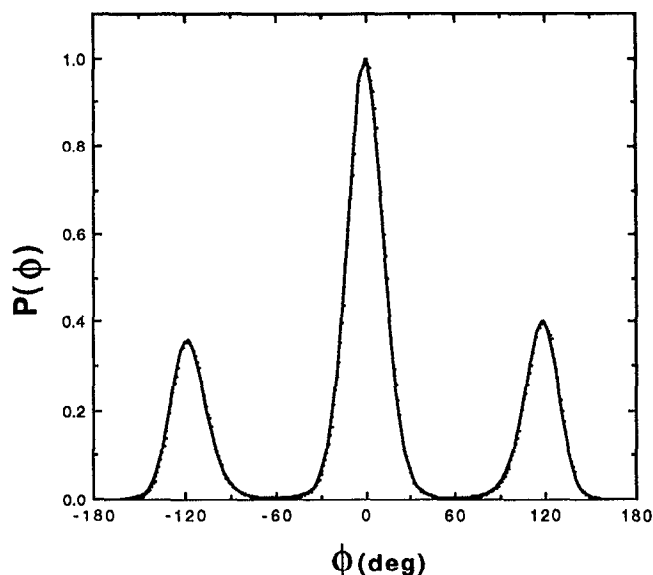


FIG. 2. Unnormalized probability distribution for the dihedral angles, measured relative to $\phi = 0^\circ$ for a *t* state, for internal C–C bonds at 400 K. The largest probability is arbitrarily assigned a value of one.

For a quantitative analysis, the dihedral angle ϕ_i ($i = 2, n - 1$) defined by the instantaneous state of the *i*th internal C–C bond is assigned to a rotational isomeric state as $|\phi_i| < 30^\circ = t$ and $\pm 90^\circ < \phi_i < 135^\circ = g^\pm$. Very rapid oscillations of unusually large magnitude, or transitions from one rotational isomeric state to another, sometimes lead to values of ϕ_i that lie outside these ranges. We assign to such values the last definite rotational isomeric state. Since the time spent in these transition regions is extremely short (less than 0.1 ps) compared with the time scale (0.1 ns) of rotational isomeric transitions, the uncertainty introduced by this procedure is negligible.

III. CORRELATIONS IN TRANSITIONS AT NEARBY BONDS

Figure 3 depicts the occurrence of 2482 rotational isomeric transitions observed in $C_{50}H_{102}$ over a period of 3.7 ns at 400 K. Transitions occur at all of the internal C–C bonds. Correlations are not immediately obvious when all of the data is presented in the manner of Fig. 3.

Since correlations were observed in transitions at bond *i* and bond $i \pm 2$ in the Brownian dynamics simulations of a simpler chain by Helfand and co-workers,⁹ we searched for similar correlations in the molecular dynamics simulation of the atom-based model of polyethylene. This search can be made in a visual manner by suppressing the plotting of selected rotational isomeric transitions in Fig. 3. Specifically, a point representing a rotational isomeric transition by bond *i* at time *t* in Fig. 3 is suppressed unless there is also a transition at bond $i \pm j$ within the time period $t \pm \Delta t$. Figures 4 and 5 depict the result of this selection process for the case where Δt is 1 ps and $j = 1$ (Fig. 4) or $j = 2$ (Fig. 5). Figure 5 contains more points than does Fig. 4. Hence there is a stronger correlation of transitions at next nearest neighbor bonds than at nearest bonds when the pair of bonds is moni-

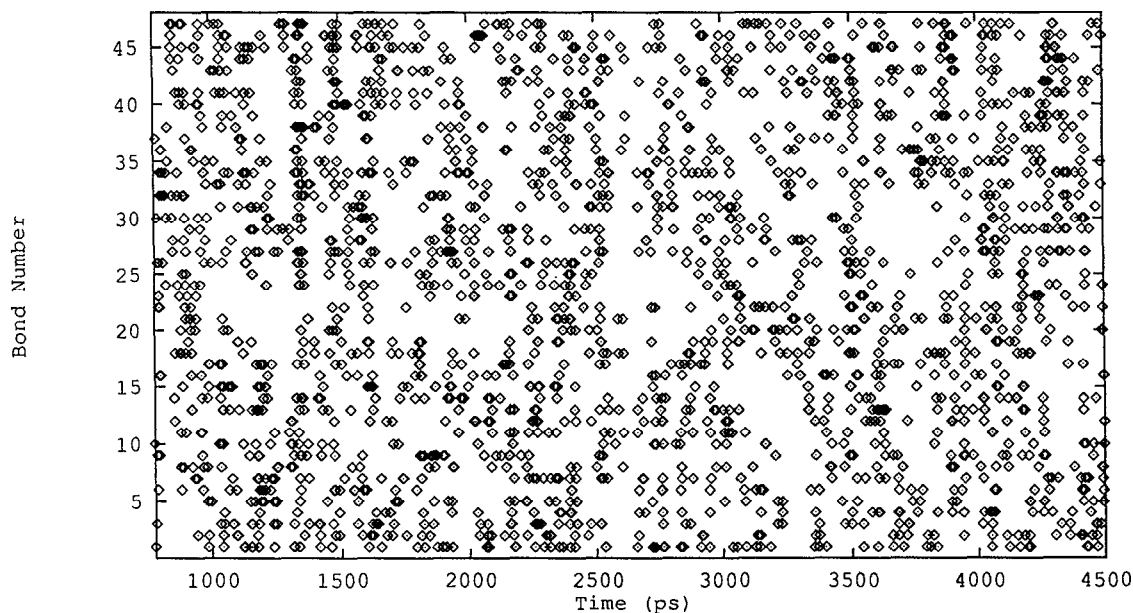


FIG. 3. Occurrence of 2482 rotational isomeric transitions in a 3.7 ns trajectory at 400 K for $C_{50}H_{102}$.

tored for 1 ps. Only 9% of the points plotted on Fig. 3 are also plotted on Fig. 4, and 18% of the points on Fig. 3 are found on Fig. 5.

Figure 6 summarizes this type of analysis for four selections of j (1, 2, 3, and 10), and for values of Δt that range from 0.2 to 2 ps. At all of these times the strongest correla-

tions are those between bonds that are next nearest neighbors. This correlation is also evident in the hazard plot (Fig. 7) of the type employed by Helfand.⁹ In fact, the dominance of the next nearest neighbor correlation in the hazard plot depicted in Fig. 7 is reminiscent of that depicted in Fig. 4 of Helfand *et al.*¹⁰ The qualitative similarity in these two haz-

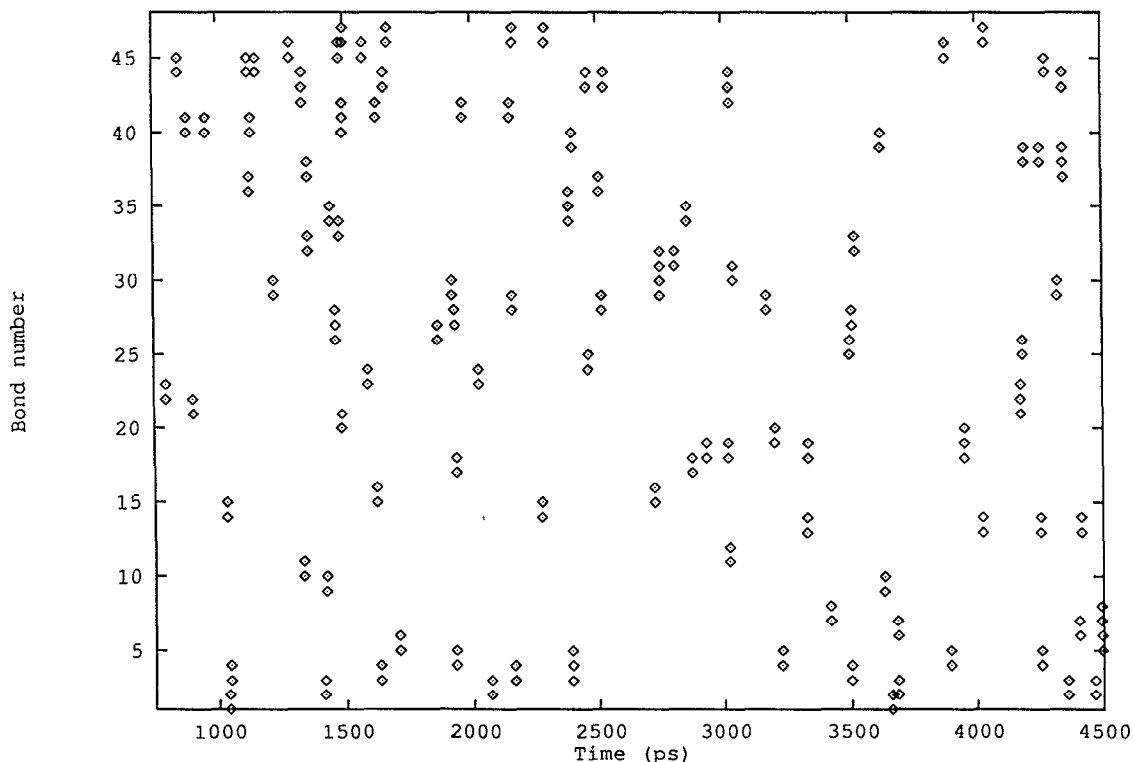


FIG. 4. Rotational isomeric transitions where there is also a transition at bond $i \pm 1$ within ± 1 ps of the transition at bond i . The figure depicts 9% of the 2482 transitions from Fig. 3.

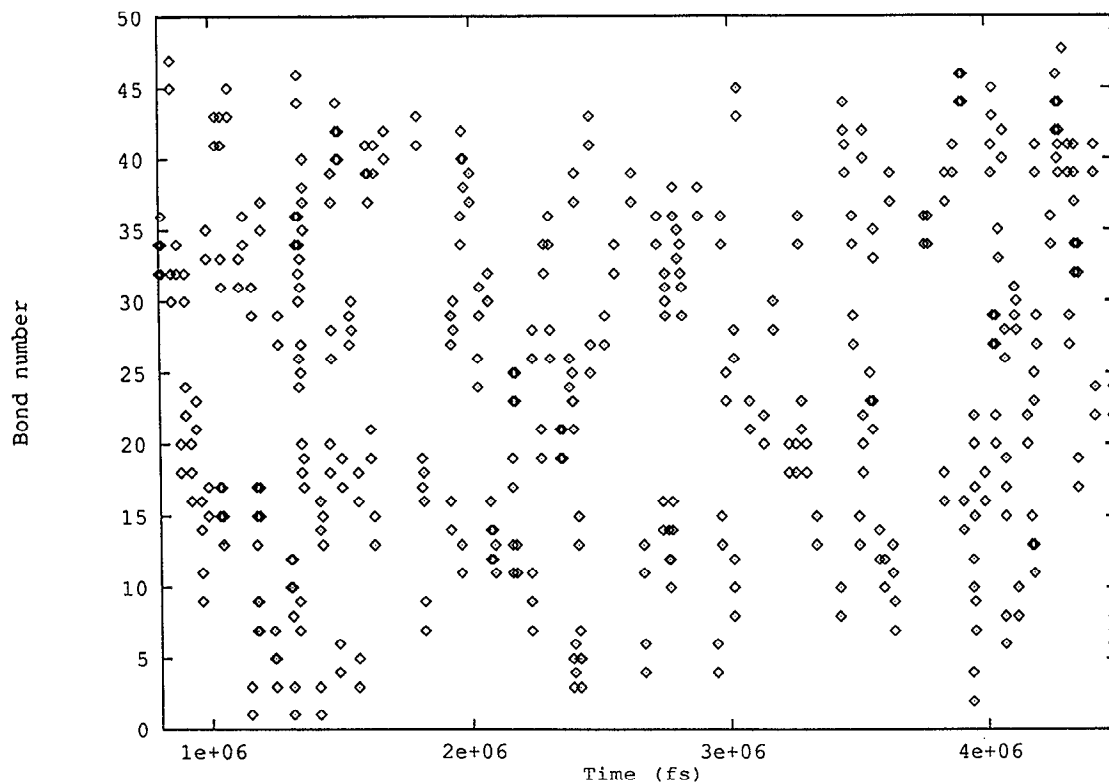


FIG. 5. Rotational isomeric transitions where there is also a transition at bond $i \pm 2$ within ± 1 ps of the transition at bond i . The figure depicts 18% of the 2482 transitions from Fig. 3.

ard plots shows that the Brownian dynamics simulations of Helfand and co-workers and the molecular dynamics simulations in the present work yield much the same type of internal dynamics.

In describing the dynamics of rotational isomerism in a chain such as polyethylene, how much emphasis should be

placed on the next nearest neighbor correlations revealed in the hazard plot in Fig. 7, and in the representation of the data by Fig. 6? After all, these two figures clearly show that there are also pairs of transitions at nearest neighbor bonds, and at bonds i and $i \pm 3$. Furthermore, the dominance of next nearest neighbor correlations ($j = 2$) over the correlations

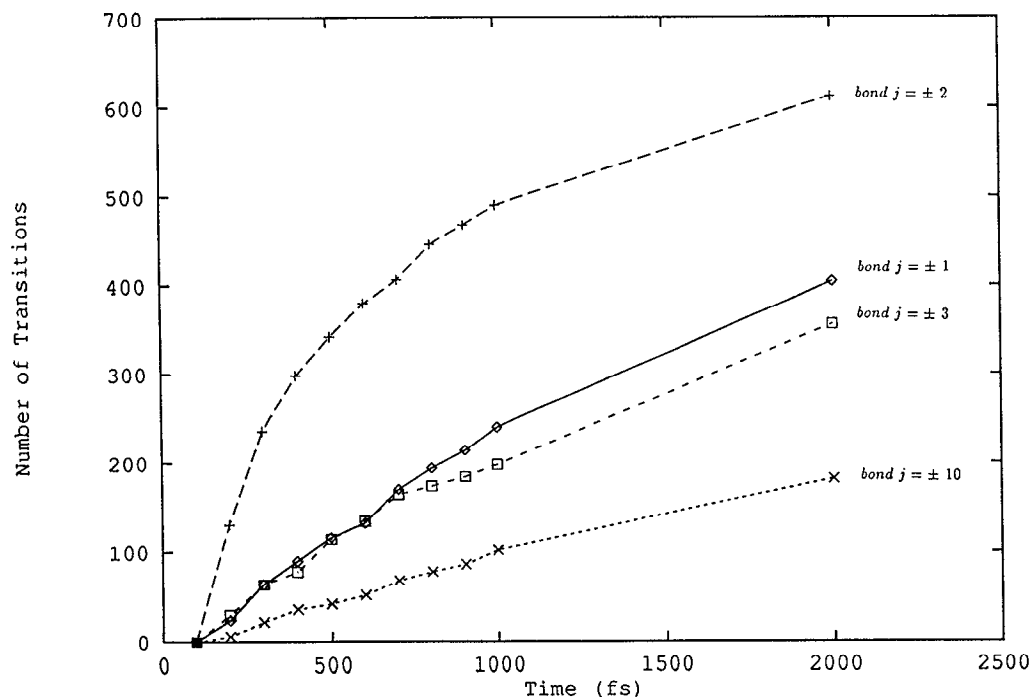


FIG. 6. Number of transitions at bond i such that there is also a transition at bond $i \pm j$ within $\pm \Delta t$ of the transition at bond i .

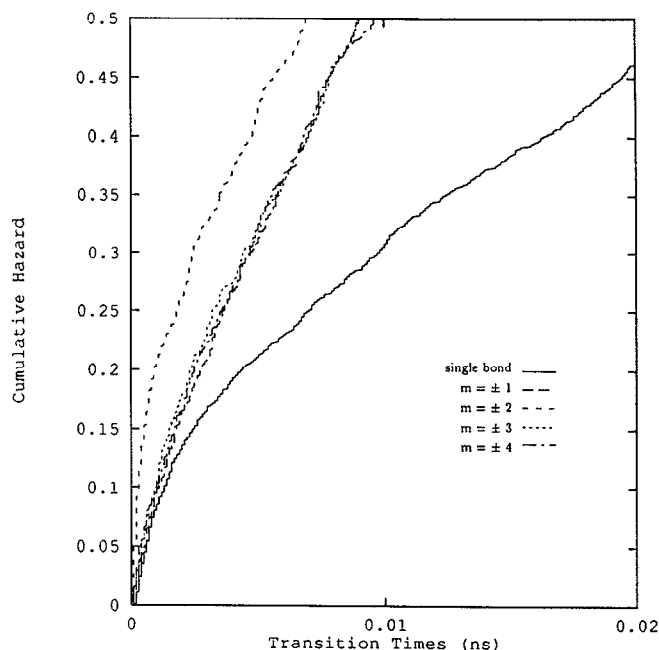


FIG. 7. The solid curve represents the cumulative hazard relating the times for a single bond undergoing a rotational transition. The other curves represent the cumulative hazard of transitions occurring m bonds away from a central bond, after that central bond has undergone a transition. This plot, constructed from the 2482 transitions depicted in Fig. 3, is made for comparison with a similar plot by Helfand (Fig. 4 of Ref. 10).

with j of 1 or 3 decreases as Δt increases (and, correspondingly, as a larger fraction of all of the transitions is examined).

This point can be made differently by contrasting the behavior depicted in Fig. 6 with that which would have been observed if there were an absolute requirement for correlated transitions at bonds that are next nearest neighbors. An example of a chain with such an absolute requirement is poly(1,4-*trans*-butadiene) confined to the channel in crystalline perhydrotriphenylene.²³ Here the *only* rotational isomeric transitions seen in a trajectory of 70 ps duration occur as correlated *antiperiplanar*[±] \leftrightarrow *antiperiplanar*[∓] transitions at CH-CH₂ bonds that are next nearest neighbors. In terms of Fig. 6, the curve with $j = 2$ would increase with time, but the curves with $j = 1$ and with $j = 3$ would remain precisely at zero throughout the trajectory. This absolute correlation is imposed on the poly(1,4-*trans*-butadiene) chain by the walls of the channel. When the perhydrotriphenylene matrix is removed, the absolute preference for next nearest neighbor correlations is also removed.

How important is the next nearest neighbor correlation in polyethylene? One means of answering this question is to focus on N_j , which denotes the number of transitions on curve j in Fig. 6 at a particular Δt , and on N , which is the total number of transitions depicted in Fig. 3. From these data we can formulate $N_2[(N_1 + N_3)/2]^{-1}$ and $(N_1 + N_2 + N_3)N^{-1}$. The former term is the ratio of the result for $j = 2$ to the average of the results for $j = 1$ and 3, evaluated from Fig. 6 at a particular value of Δt . The latter term tells us what fraction of all of the transitions were in-

cluded in the evaluation of the former term at that particular Δt . At $\Delta t = 0.3$ ps, the number of transitions with next nearest neighbor correlations is nearly four times as large as the average of the numbers with correlations represented by $j = 1$ and 3. But these transitions account for only about 15% of all of the transitions depicted in Fig. 3. Figure 6 clearly shows that the dominance of the next nearest neighbor correlations decreases as Δt is assigned larger values. Is the strength of the next nearest neighbor correlations sufficient so that it remains evident when other types of analysis are used, which employ all of the transitions depicted in Fig. 3, rather than a carefully selected subset of the data that contains only 15% of the transitions? Alternatively stated, how well might the dynamics be approximated by a simpler analysis that ignores the next nearest neighbor correlations? This issue is examined in the next section.

IV. *TRANS* \leftrightarrow *GAUCHE* ISOMERIZATION

Here we confine attention to the subset of bonds entering the *trans* state, at any stage of the simulation, and evaluate the fraction $f(\tau)$ of bonds in the subset whose isomeric transition back to g^\pm occurs within a time period shorter than or equal to τ . Each event of residence in the *trans* state is independently analyzed, by adopting as its time origin that of passage into this state. Passages only in the forward direction of the isomerization $t \rightarrow g^\pm$ are considered in the evaluation of $f(\tau)$.

The results obtained for C₅₀H₁₀₂ at 400 K are plotted with square symbols in Fig. 8. The isomerization time τ_i associated with the passage from *trans* to either of the *gauche* states may be found by the numerical integration of the solid curve according to the general formula²⁴

$$\tau_i/2 = \int_0^\infty \frac{f(\tau) - f(\infty)}{f(0) - f(\infty)} d\tau, \quad (1)$$

which, in the present case, reduces to

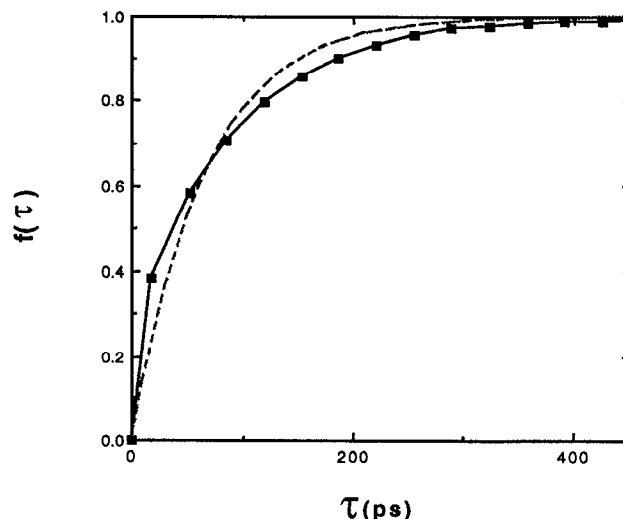


FIG. 8. Time dependence of the probability $f(\tau)$ that a bond originally in state *trans* will undergo a rotameric transition prior to time τ . The points are from the molecular dynamics trajectory for C₅₀H₁₀₂, and the dashed line is from Eq. (4), using $\tau_i = 132$ ps.

$$\tau_i = 2 \int_0^\infty [1 - f(\tau)] d\tau. \quad (2)$$

The factor of 2 in Eqs. (1) and (2) arises from the fact that the fraction $f(\tau)$ is obtained for the transition $t \rightarrow g^\pm$ whereas τ_i is defined for the transition $t \rightarrow g^+$ or $t \rightarrow g^-$, which is two times smaller. Application of Eq. (2) yields the isomerization time $\tau_i = 132$ ps. This time can be identified with the reciprocal of the rate constant k_{gt} associated with the isomerization reaction



or



as

$$\tau_i = \frac{1}{k_{gt}}. \quad (3)$$

Using the analogy to a chemical reaction, $[1 - f(\tau)]$ may be viewed as the probability that the reactant remains unchanged in the unimolecular irreversible reaction



Assuming first order kinetics and using Eq. (3), the time dependence of this probability reads

$$f(\tau) = 1 - \exp(-2\tau/\tau_i). \quad (4)$$

Figure 8 compares the results from molecular dynamics simulations and the prediction of Eq. (4), calculated using $\tau_i = 132$ ps. The data from the molecular dynamics trajectory shows a faster rise in $f(\tau)$ at small times than does the computation from Eq. (4). The two curves cross which τ is about one-half of τ_i . Equation (4) underestimates $f(\tau)$ at longer times. Thus the influence of coupled transitions at short times is apparent.

V. EQUILIBRATION

The conditional probability $p(g^\pm/t)$ evaluated from the molecular dynamics trajectory of $C_{50}H_{102}$ is depicted in Fig. 9. This conditional probability is defined as the probability that a bond in a t state at zero time is in either of the g states at a subsequent time. At long times $p(g^\pm/t)$ approaches the equilibrium probability $p^0(g^\pm) = 0.43$, as expected. The relaxation time τ_e associated with this equilibration process may be evaluated from

$$\tau_e = \int_0^\infty [1 - p(g^\pm/t)/p^0(g^\pm)] d\tau, \quad (5)$$

which follows from the application of the right-hand side of Eq. (1) to $p(g^\pm/t)$. τ_e is found to be 37 ps, which is about 3.6 times smaller than the isomerization time τ_i evaluated above.

The conditional probability $p(g^\pm/t)$ may be analytically obtained from the solution of the master equation governing conformational stochasticity.^{20,21} In the simplest case of a single bond obeying independent transitions following the scheme:

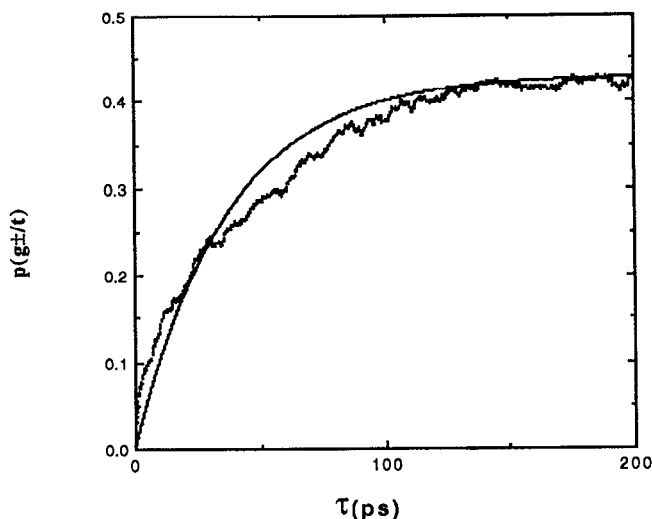
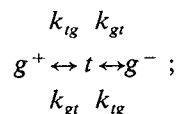


FIG. 9. Time dependence of the conditional transition probability $p(g^\pm/t)$. The dashed line is drawn with Eq. (11), and the jagged line is the result from the molecular dynamics simulation.



two modes with frequencies k_{gt} and $2k_{gt} + k_{ig}$ are operative in rotameric motions.^{20,21} The second one contributes alone to the transition from t to g^\pm . The time required for the equilibration of *trans* bonds is

$$\tau_e = \frac{1}{2k_{gt} + k_{ig}}. \quad (6)$$

Clearly, τ_e is substantially shorter than τ_i . For stationary processes, using the principle of detailed balance, we have

$$\frac{k_{gt}}{k_{ig}} = \frac{p^0(g^+)}{p^0(t)} = \frac{p^0(g^-)}{p^0(t)}. \quad (7)$$

On the premises of single bond dynamics dominating the observed behavior, the ratio of the time constants for the equilibration and isomerization processes becomes

$$\frac{\tau_i}{\tau_e} = 2 + \frac{p^0(t)}{p^0(g^-)}. \quad (8)$$

From Eq. (2) and Fig. 8 we have $\tau_i = 132$ ps, and from Eq. (5) and Fig. 9 we have $\tau_e = 37$ ps, yielding $\tau_i/\tau_e = 3.6$. From the long time limit in Fig. 9, $p^0(t)/p^0(g^-) = 2.7$ and $2 + p^0(t)/p^0(g^-) = 4.7$. The ratio of τ_i to τ_e is predicted to within 25% of the correct value by an analysis that completely ignores the cooperativity of the rotational isomeric transitions. The smooth curve in Fig. 9 is the single exponential

$$p(g^\pm/t) = p^0(g^\pm) [1 - \exp(-\tau/\tau_e)], \quad (9)$$

where the best fitting value $\tau_e = 37$ ps is used. The value of $p(g^\pm/t)$ obtained directly from the molecular dynamics trajectory rises slightly faster than the smooth line at times up to one-half of τ_e , perhaps reflecting the influences of next nearest neighbor correlations that are important at very short times. Nevertheless, the smooth curve does follow the

TABLE I. Values for k_{gt} from simulations at 300 K.

Carbon atoms	$2 k_{gt}$ (ns ⁻¹)	Reference
C4	7.6	7
C4	15.5	11
C7	4.7	7
C10	7.5	11
C10	4.0	This work
C50	2.5	This work
C200	1.6	10

data closely enough so that a useful summary of the equilibration time is provided by Eq. (9).

VI. COMPARISON WITH OTHER RESULTS

In order to compare the results obtained from CHARMM with others in the literature we have calculated a trajectory for $C_{50}H_{102}$ at 300 K. The results for the transition rate $2k_{gt}$ are presented in Table I. The value for $C_{10}H_{22}$ is the result of a trajectory run at 400 K and then scaled to the value it should have at 300 K if $C_{10}H_{22}$ follows the same exponential law as $C_{50}H_{102}$. In the table are also listed published values obtained from other simulations. In spite of the differences in the algorithms used, the results are in quite good agreement. Isomerization times of 7.6 and 4.7 ns are reported by Levy *et al.*⁷ for C4 and C7, respectively, while Helfand's Brownian simulations¹⁰ yield a value of 1.61 ns for C200. The times 4.0 and 2.5 observed for $C_{10}H_{22}$ and $C_{50}H_{102}$ in the present simulations are consistent with those findings. Isomerization times reported by Montgomery *et al.*¹¹ lie slightly above those times.

Table II compares results deduced from molecular dynamics trajectories at 400 K for linear chains of 50 and 100 carbon atoms and for a cyclic chain with 100 carbon atoms. The same characteristic time is reported in the two rows, but computed in different ways. The first row is the isomerization time obtained through Eq. (5), and multiplying by 4.7

TABLE II. Comparison of two linear chains and one cyclic chain. All times are in ns.

Property	$C_{50}H_{102}$	$C_{100}H_{202}$	$C_{100}H_{200}$
$4.7 \tau_c$	0.166	0.164	0.163
$1/k_{gt}$	0.166	0.182	0.171

according to Eq. (8). The final row lists the inverse of the transition rate which is obtained as the ratio of the number of t to g^\pm transitions and the total time spent in the *trans* state. The data in Table II shows that the molecular dynamics is not sensitive to a doubling in the number of carbon atoms from 50 to 100, nor are the transition times for a chain of 100 carbon atoms affected significantly by the presence or absence of ends. (Of course, the rates of conformational transitions do increase for much shorter linear chains, due to heavier weighting of the more mobile bonds near the end of the chain.)

ACKNOWLEDGMENTS

This research was supported by grants from the National Science Foundation (DMR 89-15025) and the Petroleum Research Fund, administered by the American Chemical Society.

- ¹C. L. Brooks III, M. Karplus, and B. M. Pettitt, *Adv. Chem. Phys.* **71**, 1 (1988).
- ²M. Fixman and J. Kovac, *J. Chem. Phys.* **61**, 4939 (1974).
- ³J. P. Ryckaert and A. Bellemans, *Faraday Discuss. Chem. Soc.* **66**, 95 (1978).
- ⁴M. Fixman, *J. Chem. Phys.* **69**, 1527 (1978).
- ⁵T. A. Weber, *J. Chem. Phys.* **69**, 2347 (1978).
- ⁶T. A. Weber, *J. Chem. Phys.* **69**, 4277 (1978).
- ⁷R. M. Levy, M. Karplus, and J. A. McCammon, *Chem. Phys. Lett.* **65**, 4 (1979).
- ⁸G. T. Evans and D. C. Knauss, *J. Chem. Phys.* **71**, 2255 (1979).
- ⁹E. Helfand, Z. R. Wasserman, and T. A. Weber, *J. Chem. Phys.* **70**, 2016 (1979).
- ¹⁰E. Helfand, Z. R. Wasserman, and T. A. Weber, *Macromolecules* **13**, 526 (1980).
- ¹¹J. A. Montgomery, Jr., S. L. Holmgren, and D. Chandler, *J. Chem. Phys.* **73**, 3688 (1980).
- ¹²W. F. van Gunsteren, H. J. C. Berendsen, and J. A. C. Rullmann, *Mol. Phys.* **44**, 69 (1981).
- ¹³B. R. Brooks, R. E. Bruccoleri, B. D. Olafson, D. J. States, S. Swaminathan, and M. Karplus, *J. Comput. Chem.* **4**, 187 (1983).
- ¹⁴P. A. Wielopolski and E. R. Smith, *J. Chem. Phys.* **84**, 6940 (1986).
- ¹⁵R. Edberg, D. J. Evans, and G. P. Morriss, *J. Chem. Phys.* **84**, 6933 (1986).
- ¹⁶R. Edberg, G. P. Morriss, and D. J. Evans, *J. Chem. Phys.* **86**, 4555 (1987).
- ¹⁷S. Karaborni and J. P. O'Connell, *J. Chem. Phys.* **92**, 6190 (1990).
- ¹⁸Polygen Corp., 200 Fifth Avenue, Waltham, Massachusetts 02254.
- ¹⁹A. Abe, R. L. Jernigan, and P. J. Flory, *J. Am. Chem. Soc.* **88**, 631 (1966).
- ²⁰R. L. Jernigan, in *Dielectric Properties of Polymers*, edited by F. E. Karasz (Plenum, New York, 1972), p. 99.
- ²¹I. Bahar and B. Erman, *Macromolecules* **20**, 1368 (1987).
- ²²I. Bahar, I. Zúñiga, R. Dodge, and W. L. Mattice, *Macromolecules* **24**, 2986 (1991).
- ²³R. Dodge and W. L. Mattice, *Macromolecules* **24**, 2709 (1991).
- ²⁴B. J. Berne and R. Pecora, *Dynamic Light Scattering* (Wiley, Interscience, New York, 1976).